Progress In Electromagnetics Research M, Vol. 117, 151–161, 2023

Design of a Beam-Steering Metamaterial Inspired LPDA Array for 5G Applications

Rania Eid A. Shehata[1, 2, *], Moataza Hindy[2], Hamdi Elmekati[1], and Ayman Elboushi[2]

Abstract—This article presents the design and implementation of a beam-steering antenna array using a 4×4 Butler matrix feed network (BMN) for 5G applications. The proposed antenna array can achieve a gain of 14 dBi and a steering range of ($+16°$, $-47°$, $+46.5°$, $-15.7°$) to cover angular range extending from $45°$ to $135°$. To achieve that, a simple, 4×4 Butler matrix etched on a single-layer microstrip structure is designed, optimized, and fabricated. The proposed design incorporates phase shifters, 3-dB couplers, and cross-over couplers. The proposed matrix is employed as a feeding network for 4-element wideband LPDA antenna array. The fabrication results of the feeding matrix and antenna array show very good agreement with the simulated results.

1. INTRODUCTION

Nowadays, a rapidly increasing rate of growth is being seen in the demand for larger capacity and higher data rates in wireless communication worldwide [1–3]. Therefore, millimeter-wave frequency (MMW) bands could be considered as a perfect candidate for the investigation of such a system. However, because oxygen molecules in the propagation environment absorb waves, the MMW frequency bands experience extremely significant attenuation [4, 5]. So, the need for high gain antenna array with proper radiation characteristics becomes an urgent demand. Nowadays, the technology of smart antennas is based on switched beam systems. Multiple fixed beams are created by an antenna array system with more sensitivity in a specific area. This array system exposes signal strength, selects one of the several fixed beams, and switches from one beam to another for tracking moving users. One of the most important parts of a switched beam antenna system is the feeding of the network [6]. Moreover, Beamforming techniques can be adopted to enhance the signal-to-noise ratio (SNR) of received signals, eliminate undesirable interference from the unwanted sources, and focus the transmitted signals to specific areas. The beamformed array can generate multiple beams in an angular area, enhancing capacity as it can cover multiple users with different beams [7, 8]. In a beamforming network design, eligible features are simplicity, low design costs, low losses, and most significantly, compact size and simple antenna integration to decrease the number of components. The Butler matrix-fed network (BMN) has become more popular than other beamforming techniques such as the Nolen matrix [9], Rotman lens [10], and Blass matrix [11], because it contains the simplest components and has, theoretically, much lower lossless. Furthermore, an $N \times N$ Butler matrix is a network with N inputs and N output ports such that for every input port, signals with congruous power and advanced phase shifts are created in the output ports. So, at the outputs of the matrix, N orthogonal beams are generated [12].

In [13], the antenna elements and Butler matrix are designed using microstrip technology, but no switches are integrated. It should be noted that they must connect extra 50-termination loads for the three unused Butler matrix ports during the test. In [14, 15], a complex and costly structure of a 1×4

Received 24 April 2023, Accepted 14 June 2023, Scheduled 1 July 2023

* Corresponding author: Rania Eid A. Shehata (rania.eid@eri.sci.eg).

[1] Electronics and Communication Engineering Department, Mansoura University, Cairo, Egypt. [2] Microstrip Department, Electronics Research Institute, New Nozha, Cairo, Egypt.

microstrip antenna, a 4×4 Butler matrix, and a packaged switch chip is mounted on a planar PCB and housed in a metal enclosure. This work proposes a simpler structure, with proper overall performance. Compared to other designs adopting substrate integrated waveguide (SIW) technology, the proposed design is implemented using microstrip technology, which is easier to integrate with other components in systems, and there is no need for a SIW to microstrip transition. The antenna element employed in this steering array is based on the design presented in [4]. This design represents a log periodic dipole array (LPDA) loaded epsilon near zero (ENZ) metamaterial which satisfies the requirements for the proposed steering array in terms of directivity, impedance bandwidth, and radiation characteristic. This work presents the simplest solution of multi-beam antenna arrays with Butler matrices with a compact size.

2. SINGLE ELEMENT DESIGN

2.1. Metamaterial with Epsilon Near Zero Index

The phase velocity of electromagnetic waves that are propagating tends to infinity in ENZ metamaterials. The effect is that the ultimate wavelength also approaches infinity. As a result, in this case, the fields at the two ends of a slab of an ENZ metamaterial are nearly similar. This characteristic plays an important role in antennas [16]. To create a restricted pattern with strong directivity, the metamaterial is used as a high refractive index impact. The metamaterial's high refractive index effect is intended to replace dielectric lenses for gain augmentation. According to Fig. 1, the unit cell is created in Computer Simulation Technology Microwave Studio (CST MWS) and simulated utilizing perfect electric conductor (PEC) and perfect magnetic conductor (PMC) boundary conditions in the yz and xy axes. The unit cell gets excited on the y-axis. In Table 1, the planned ENZ unit cell's optimized dimensions are listed. The unit cell's substrate is made of Rogers 5880, which has a loss tangent of 0.0009, a thickness of 0.254 mm, and a relative permittivity of 2.2. The PEC and PMC border conditions around the unit cell are used to mimic it in CST MWS. The recovered properties from [17], including permeability, refractive index, and effective permittivity, are shown in Fig. 1. Based on Fig. 2, the permittivity at the frequency range of 26–39 GHz is less than unity. The antenna's gain can be improved by focusing the E-filed from the LPDA through this area after printing the array of unit cells; this will boost the antenna's gain.

Table 1. Optimized dimensions of unit cell [4].

Symbol	Value (mm)
A	0219
B	0.76
R	0.5

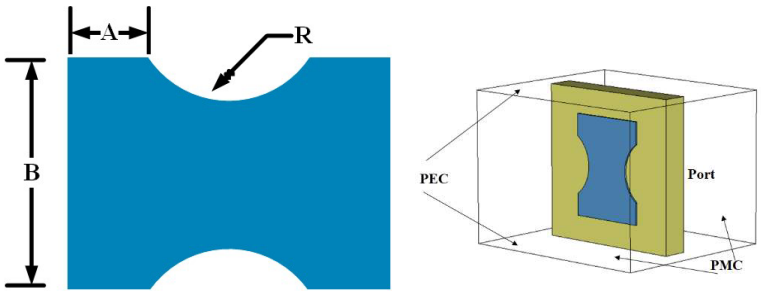

Figure 1. Schematic diagram of the ENZ unit cell [4].

2.2. Convex Rows of Loaded LPDA (CXRL LPDA)

A wideband single LPDA element antenna loaded with ENZ index metamaterial is designed and optimized to operate at the proposed frequency of 28 GHz. The consecutive five arms of the LPDA antenna element were structured on an RO5880 substrate, which has a loss tangent of 0.0009, a thickness of 0.254 mm, and a relative permittivity of 2.2. The fabricated layout and schematic diagram are shown

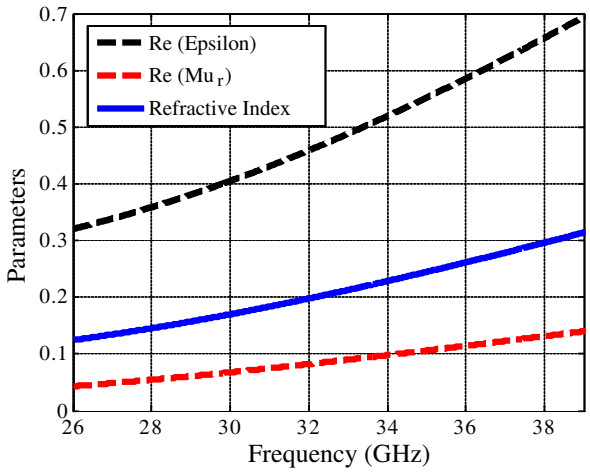

Figure 2. Characteristics of the unit cell: refractive index (n), permittivity and permeability [4].

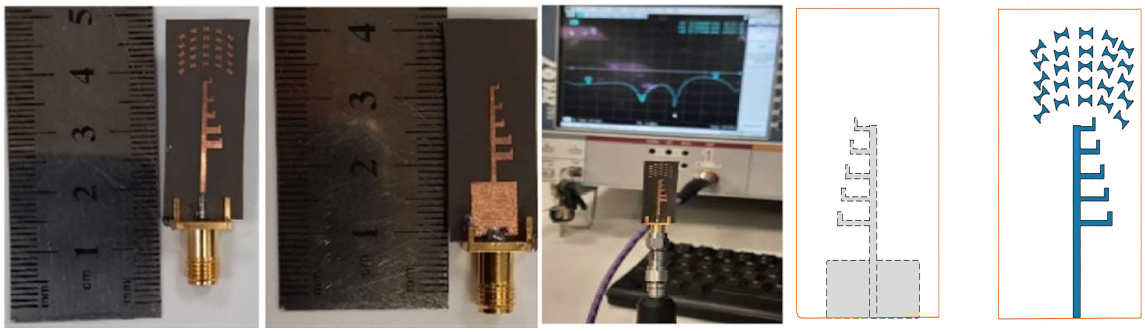

Figure 3. Prototype of fabricated and Schematic diagram CXRL LPDA [4].

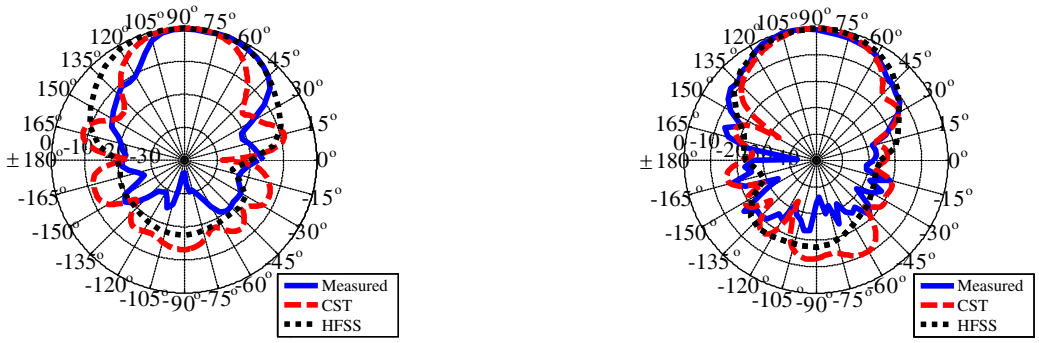

(a) E-plane (28 GHz) (b) H-plane (28 GHz)

Figure 4. Simulated and measured 2D radiation pattern of CXRL LPDA [4].

in Fig. 3. The proposed design dimensions and simulated return loss S_{11} were presented in [4]. Fig. 4 displays the antenna's measured and simulated 2D radiation patterns in the E- and H-planes at 28 GHz.

3. BUTLER MATRIX DESIGN

BMN is chosen as a feeding network for the LPDA array elements with a view to producing orthogonal beams that can be directed in various directions. Fig. 5 presents 4×4 BMN schema, in which the steerable beams are indicated to the thrilling input port. This BMN has 4 input ports and 4 output ports, where the proposed radiating array elements are attached to the 4 output ports. According to the schematic diagram, the branch line coupler, crossover, and phase shifter are the significant elements of a BMN. All those elements are simulated, optimized, and fabricated on a 0.254 mm thick Rogers 5880 substrate ($\varepsilon_r = 2.2$).

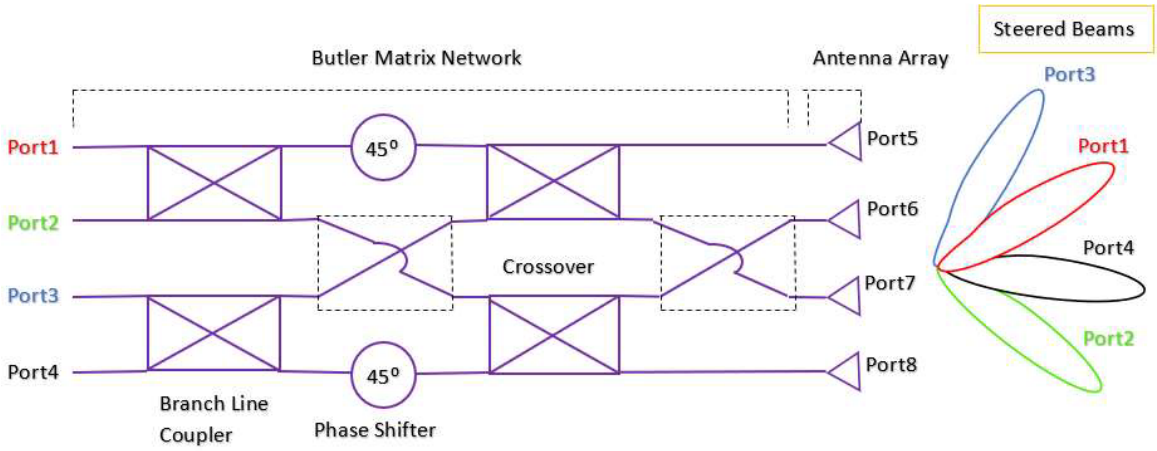

Figure 5. Schematic diagram of a 4×4 Butler matrix.

3.1. Branch Line Coupler (BLC)

BLC is an essential passive component of the BMN as shown in Fig. 6(a). A hybrid coupler is also described as a 3 dB coupler where power is transmitted equally among all output ports with a 90 degree phase difference at the desired frequency. The S-parameters at 28 GHz ($S_{11} = -29.363$ dB, $S_{21} = -3.43$ dB, $S_{31} = -3.45$ dB, and $S_{41} = -36.92$ dB), and the phase difference between port 2 and port 3 (89.99°) are reported in Figs. 6(b) and (c). The line impedances are calculated by the following Eqs. (1) and (2) [18]

$$W = \frac{8he^B}{e^{2B} - 2} \tag{1}$$

$$B = \frac{Z0}{60} * \sqrt{\frac{\varepsilon_{r+1}}{2}} + \frac{\varepsilon_{r-1}}{\varepsilon_{r+1}} \left(0.23 + \frac{0.11}{\varepsilon_r}\right) \tag{2}$$

where W = Width of the line; h = height of the substrate, which is 0.254 mm; ε_r = Primitivity of the substrate, which is 2.2.

3.2. Crossover (0 dB)

Crossover is the supplementary element utilized in the BMN, as illustrated in Fig. 7(a). The crossover is designed with a high level of isolation between the input ports, to prevent overlapping signals during crossings. The obtained S-parameters at 27.9 GHz ($S_{31} = -0.31$ dB, $S_{11} = -65.645$ dB) are presented in Fig. 4(b).

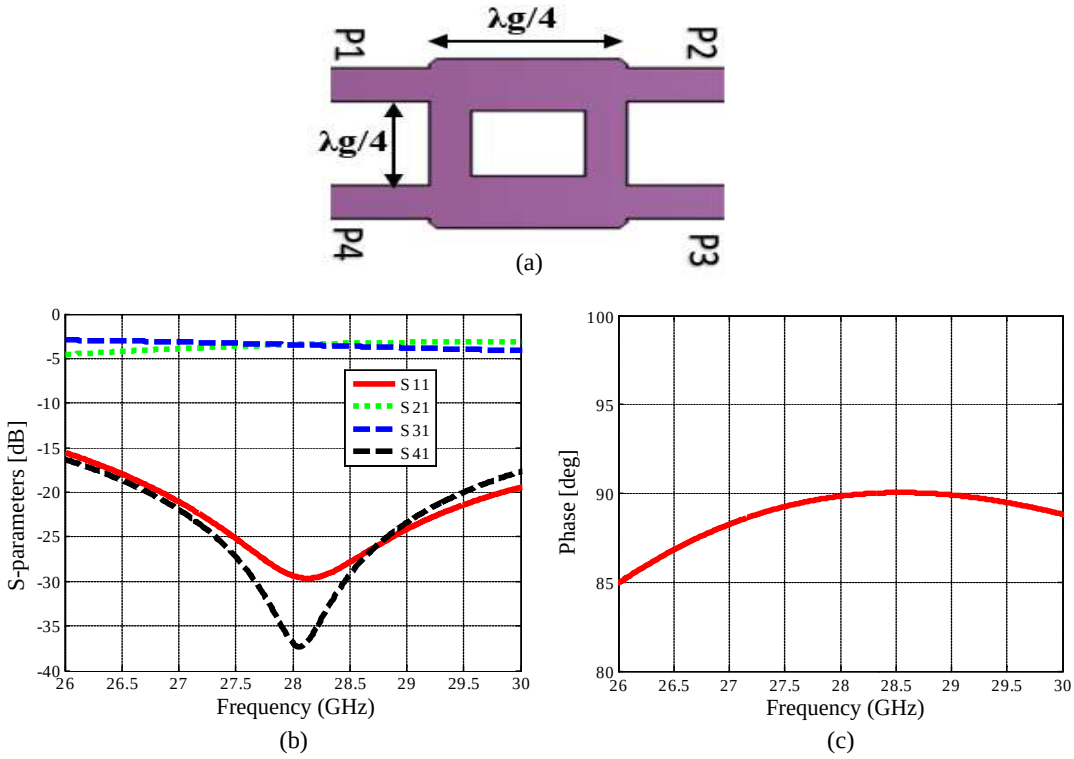

Figure 6. (a) Schematic diagram of BLC. (b) S-parameter of BLC. (c) The phase difference between the output ports of BLC.

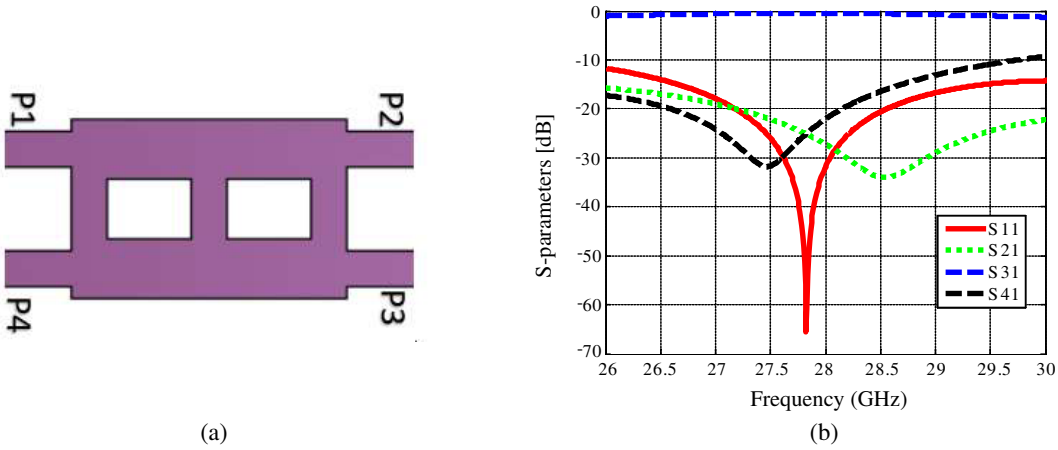

Figure 7. (a) Schematic diagram of the proposed cross-over. (b) S-parameters of crossover.

3.3. Phase Shifter

A phase shifter is another critical component employed in the BMN that modifies the wave's phase angle [19]. The designed 45° microstrip phase shifter is illustrated in Fig. 8(a), and its output phase shift at 28 GHz (45°) is presented in Fig. 5(b). The length ΔL in Fig. 5(a) is calculated by Eq. (3):

$$\Delta L = 2 * \theta * \lambda g/360 \tag{3}$$

where λg: Guided Wavelength. θ: Desired Phase shift (45°).

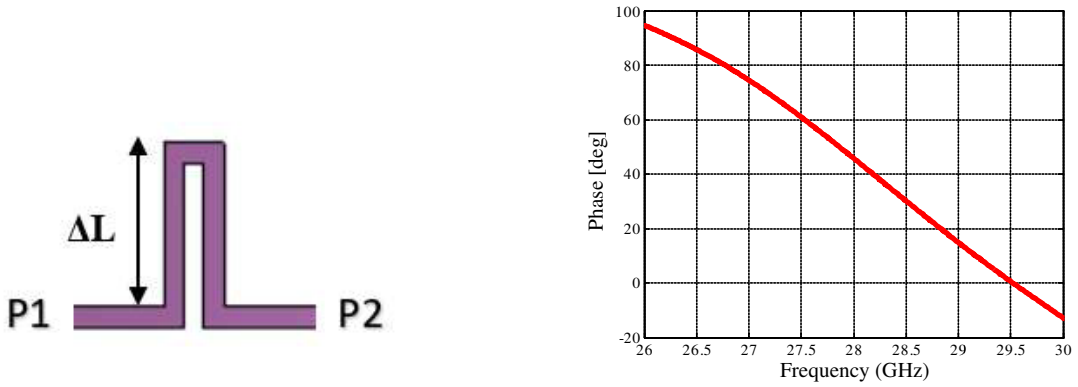

(a) (b)

Figure 8. (a) Schematic diagram of a Phase shifter 45°. (b) The Output Phase of Phase Shifter.

3.4. 4 × 4 Butler Matrix

A 4 × 4 BMN structure is designed by integrating all of the sections described above. It comprises four inputs and four outputs that are coupled by BLCs, crossovers, and phase shifters. When a signal is delivered to any port, it is divided equally with a sequential phase shift and an equal magnitude among the four output ports. The schematic diagram of Butler matrix is shown in Fig. 9(a). It consists of two 45° phase shifters, two crossovers, and four BLCs. The outputs of the first two BLCs are fed to phase shifters and crossovers to give the necessary phase shifts without signal overlapping.

Figure 9(b) illustrates the simulated and measured S-parameters for the BMN. The results indicate that at 28 GHz, the reflection coefficients (S_{11}, S_{22}, S_{33}, and S_{44}) are −15 dB. The insertion loss magnitudes (S_{51}, S_{61}, S_{71}, S_{81}, S_{52}, S_{62}, S_{72}, S_{82}, S_{53}, S_{63}, S_{73}, S_{83}, S_{54}, S_{64}, S_{74}, and S_{84}) have approximately values (−6 dB), as shown in Fig. 9(c).

As previously indicated, the basic target of BMN is to steer the antenna beam by gradually increasing the phase difference between the successive output ports. The selection of suitable input ports permits the phase difference to be achieved on each output port. When the input is applied to port 1, the output port's progressive phase difference is −45°. Also, when the input is applied to ports 2, 3, and 4, the phase differences are, respectively, +135°, −135°, and +45°.

Figure 9(d) illustrates the simulated and measured phase differences for the output ports of the 4 × 4 BMN at 28 GHz. The ideal progressive phase differences between (S_{61} & S_{51}, S_{71} & S_{61}, and S_{81} & S_{71}) should have been −45°. As shown in Fig. 6(d), the acquired average phase is −46.29° with an error 1.29°. The different average output phases detected for excitations at ports 2, 3, and 4 are 134.066°, −136°, and 46.766°. Table 2 shows acceptable values of the phase errors produced by successive out ports.

Table 2. The simulated phase differences between the butler matrix output ports.

Input Port	Obtained phase at Output Ports (°)			Average Phase (°)	Theoretical Target (°) (β)	Phase Error (°)	Phase Error %
	5–6	6–7	7–8				
1	−49.67	−43.65	−45.55	−46.29	−45	1.29	0.5805
2	132	132.2	138	134.066	135	0.94	1.269
3	−138	−132	−128	136	−135	1	1.35
4	45.47	44.94	49.89	46.766	45	1.766	0.7947

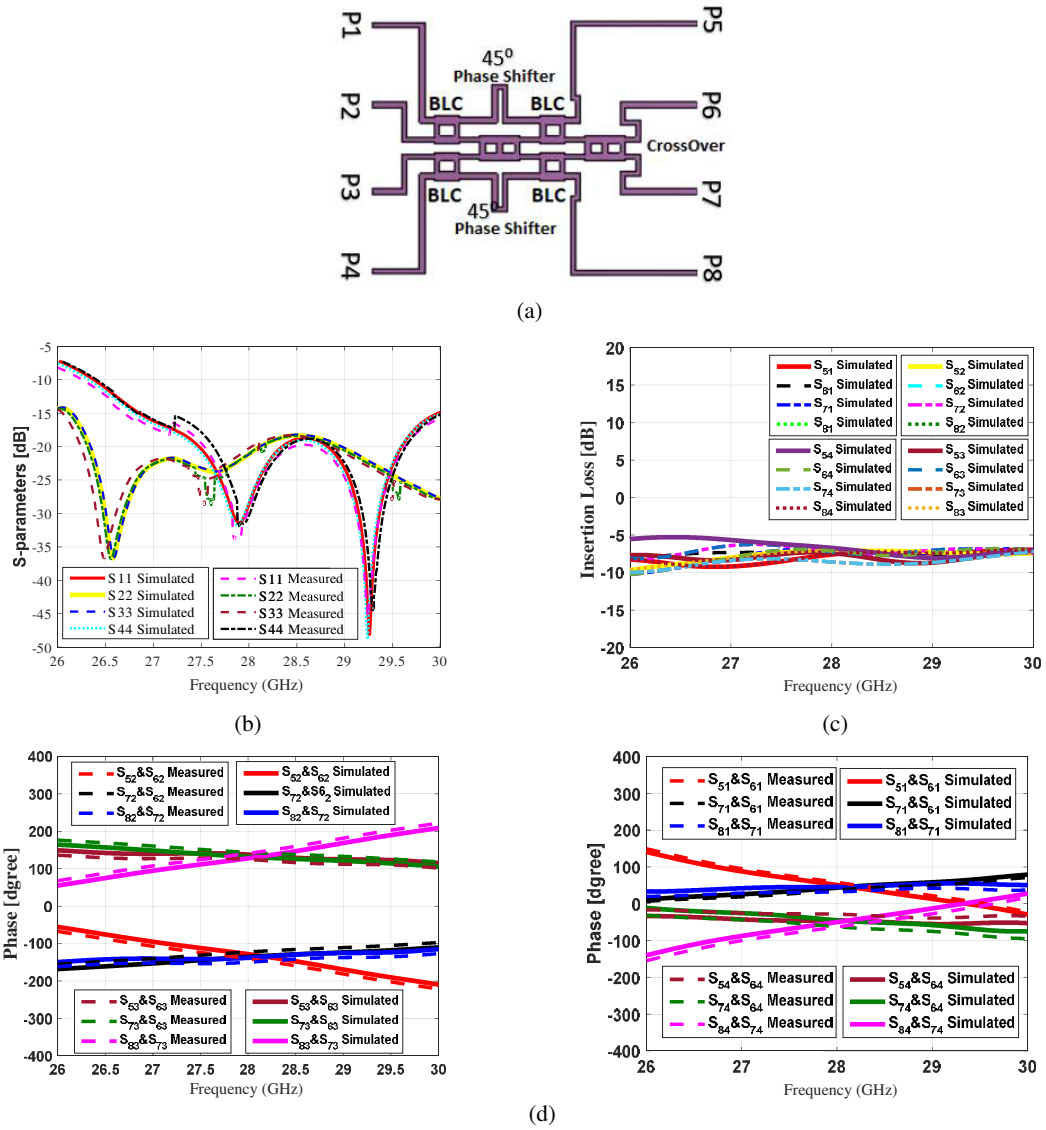

Figure 9. (a) Designed 4×4 BMN and. (b) Reflection Coefficient of 4×4 BMN. (c) The simulated Insertion loss between input and output ports. (d) The simulated progressive phase differences.

3.5. Butler Matrix with an Antenna Array

In this section, the results of the proposed design are obtained by using the Advanced Design System (ADS 2019) simulator to show return loss for input ports. The data is extracted from CSTMWS (Touchstone files) and used to obtain results in ADS, as shown in Fig. 10(a). The results were presented in Fig. 10(b) and compared with the measured ones. The results obtained by ADS are in good agreement with the measured results.

The return Losses are measured using Vector Network Analyzer VNA (ROHDE & SCHWARZ ZVA 67) after calibrating it using the standard calibration kit. The fabrication of a four-element antenna array is shown in Figs. 11(a)–(b). The proposed array system can operate at 28 GHz, covering a band extending from 26.5 GHz to 30.5 GHz, and is fed by a 4×4 Butler matrix feed network. Both the BMN and the antenna array elements are designed and fabricated on a Rogers 5880 substrate with a thickness of 0.254 mm. The overall dimensions of the proposed feeding network (BMN) of beam steering antenna are 40 mm $\times$ 46 mm $\times$ 0.254 mm and after adding antennas are 120 mm $\times$ 46 mm $\times$ 0.254 mm.

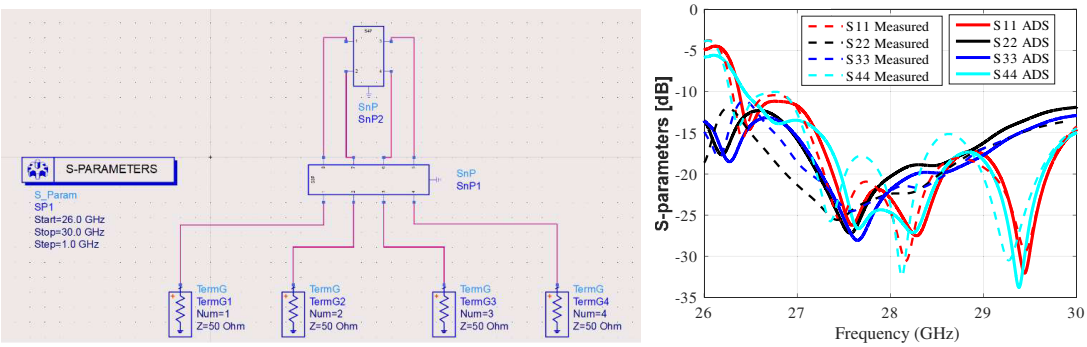

(a) (b)

Figure 10. (a) The designed system diagram in the ADS 2019. (b) S-parameters of the system.

(a) (b)

Figure 11. (a) Fabricated array system Prototype. (b) Measurement setup.

3.5.1. Discussion of the Results of the System Design

In this section, by using the practical realization of the setup with the antenna under test (AUT), the radiation patterns of the fabricated and simulated BMNs according to the input port excitations are displayed in Figs. 12(a), (c), and (d). At 28 GHz, the simulated beam orientations are $+16°$, $-46°$, $+47°$, and $15.7°$. The output gain ranges from 11.94 dBi to 14.01 dBi for each excitation input port (1 to 4), respectively, as shown in Fig. 12(b). Using the progressive phase difference (β) between the successive output ports, the beam steering angle (θ_0) can be calculated by Eq. (4) [20]:

$$\theta_0 = \sin^{-1} \frac{\beta\lambda}{2\pi d} \tag{4}$$

where β = progressive phase difference between BMN outputs (i.e., $\pm 45°$ and $\pm 135°$s); λ = wavelength at the desired frequency (28 GHz); d = distance between the antenna array elements ($\lambda g/2$).

Table 3 displays the theoretical beam steering angle (θ_0) and associated Progressive Phase Difference (β) for a 4×4 BMN, where 'θ_0' is calculated using Eq. (4). Table 4 shows the results of the maximum

Table 3. Theoretical phase difference and Beam steered angle of a 4×4 BMN at 28 GHz.

Port Excitatio	Progressive Phase Difference (β)	Beam steered angle (θ_0)
Port 1	$+45$	$+15$
Port 2	-135	-48.5
Port 3	$+135$	$+48.5$
Port 4	-45	-15

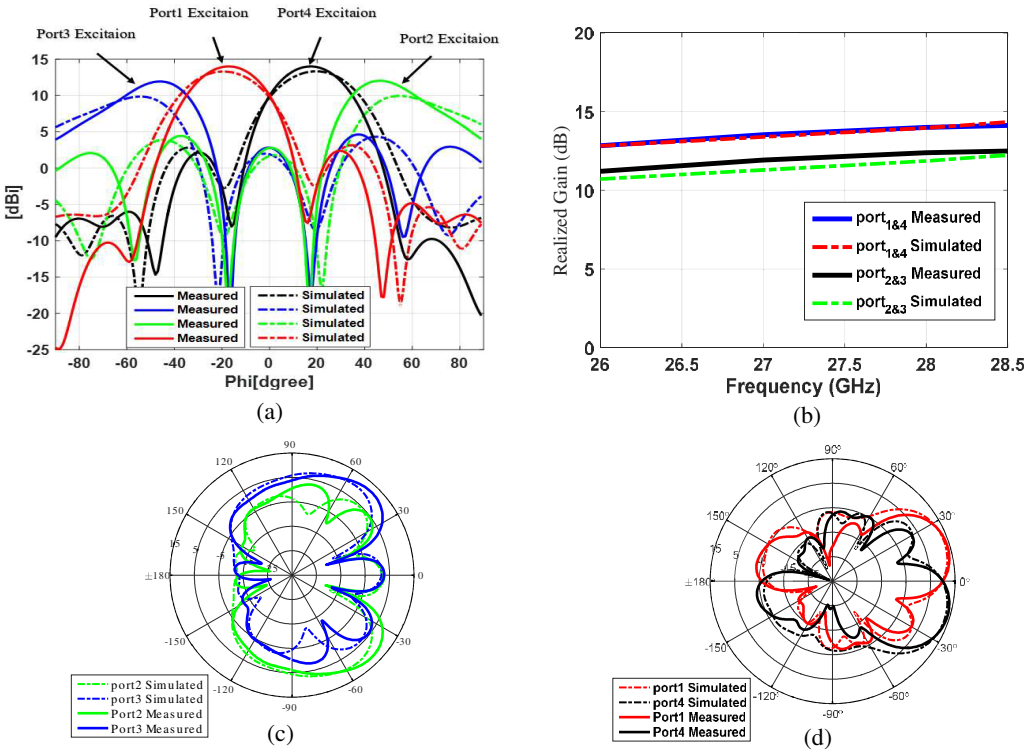

Figure 12. Measured and simulated. (a) Radiation Patterns of the proposed beam steerable antenna at 28 GHz. (b) Total realized gain. (c) Radiation Patterns for port 2 and port 3. (d) Radiation Patterns for port 1 and port 4.

Table 4. Comparison of the theoretical, simulated and measured Beam steered angles at 28 GHz.

Port Excitatio	Theoretical Beam steered angle	measured Beam steered angles	Simulated Beam steered angle	Peak Gain (dB)
Port 1	+15	+16	20	13.99
Port 2	−48.5	−46	−52	11.94
Port 3	+48.5	+47	52	12.04
Port 4	−15	−15.7	−20	14.01

Table 5. Comparison of the performances of this work with the previous works.

Ref.	Frequency (GHz)	Antenna	No. of Dielectric Layers	Butler Matrix	Maximu Beam Steerin Angle (deg)	Max. Gain (dB)	Dimensio (mm^2)
[13]	28	1 × 4 Patch	2 layer	4 × 4 Microstrip	−39°, +36°	10	36.2 × 44.3
[14]	30	1 × 6 horn	2 layer	4 × 6 Microstrip	−39°, +40°	11	95 × 32
[15]	28	1 × 4 Patch	2 layer	4 × 4 Microstrip	−43°, +34°	6.7	36 × 48
This Work	26–30	1 × 4 LPDA load by metamaterial	1 layer	4 × 4 Microstrip	−46°, +47°	14.01	35 × 40

realized gain at 28 GHz (14 dB) for the proposed antenna at 28 GHz beam steered angles of 16°, −46°, 47°, and 15.7° for the out port, and the comparison among the theoretical, simulated, and measured beam steering angles of the proposed antenna. The measured result indicates the acceptable errors of +1° for port 1, +2.5° for port 2, −1.5° for port 3, and 0.7° for port 4, compared to theoretical values. The simulated result findings demonstrate acceptable errors of ±5° for ports 1 and 4 and ±3.5° for ports 2 and 3 compared to theoretical values. According to the results described above, the proposed antenna can be used for beam steering purposes. The performance of this work compared to previous designs is summarized and tabulated in Table 5.

4. CONCLUSION

In this article, an LPDA antenna array loaded with epsilon near zero (ENZ) index metamaterial supplied by a 4×4 Butler matrix feed network is designed, simulated, optimized, fabricated, and measured. All components of the BMN are designed, simulated, and measured. There is very good agreement between measured and simulated results. This system has the advantages of high gain and multiple beam steering capabilities. The proposed array system can be considered as a good candidate for various MMWs and upper-band 5G applications operating around 28 GHz.

REFERENCES

1. Eid, R., A. Elboushi, and M. Hindy, "Wideband monopole antenna with multiple stub resonators for 5G applications," *2021 38th National Radio Science Conference (NRSC)*, Vol. 1, 80–87, IEEE, 2021.
2. Ikram, M., K. S. Sultan, A. M. Abbosh, and N. Nguyen-Trong, "Sub-6 GHz and mm-wave 5G vehicle-to-everything (5G-V2X) MIMO antenna array," *IEEE Access*, Vol. 10, 49688–49695, 2022.
3. Sultan, K., M. Ikram, and N. Nguyen-Trong, "A multiband multibeam antenna for sub-6 GHz and mm-wave 5G applications," *IEEE Antennas and Wireless Propagation Letters*, Vol. 21, No. 6, 1278–1282, 2022.
4. Shehata, R. E. A., A. Elboushi, M. Hindy, and H. Elmekati, "Metamaterial inspired LPDA MIMO array for upper band 5G applications," *International Journal of RF and Microwave Computer-Aided Engineering*, Vol. 32, No. 8, e23212, 2022.
5. Shehata, R. E. A., M. Hindy, H. Elmekati, and A. Elboushi, "Circularly polarized directive hybrid patch/horn antenna for upper band 5G applications," *Microwave and Optical Technology Letters*, 2022, DOI:10.1002/mop.33489.
6. Alam, M. M., "Microstrip antenna array with four port butler matrix for switched beam base station application," *2009 12th International Conference on Computers and Information Technology*, 531–536, IEEE, 2009.
7. Hong, W., K.-H. Baek, and S. Ko, "Millimeter-wave 5G antennas for smartphones: Overview and experimental demonstration," *IEEE Transactions on Antennas and Propagation*, Vol. 65, No. 12, 6250–6261, 2017.
8. Hong, W., Z. H. Jiang, C. Yu, et al., "Multibeam antenna technologies for 5G wireless communications," *IEEE Transactions on Antennas and Propagation*, Vol. 65, No. 12, 6231–6249, 2017.
9. Nolen, J., "Synthesis of multiple beam networks for arbitrary illuminations," Ph.D. dissertation, 1965.
10. Rotman, W. and R. Turner, "Wide-angle microwave lens for line source applications," *IEEE Transactions on Antennas and Propagation*, Vol. 11, No. 6, 623–632, 1963.
11. Mosca, S., F. Bilotti, A. Toscano, and L. Vegni, "A novel design method for Blass matrix beamforming networks," *IEEE Transactions on Antennas and Propagation*, Vol. 50, No. 2, 225–232, 2002.

12. Rahimian, A., "Microwave beamforming networks employing Rotman lenses and cascaded Butler matrices for automotive communications beam scanning electronically steered arrays," *2011 Microwaves, Radar and Remote Sensing Symposium*, 351–354, IEEE, 2011.
13. Kim, S., S. Yoon, Y. Lee, and H. Shin, "A miniaturized Butler matrix based switched beamforming antenna system in a two-layer hybrid stackup substrate for 5G applications," *Electronics*, Vol. 8, No. 11, 1232, 2019.
14. Ashraf, N., A.-R. Sebak, and A. A. Kishk, "PMC packaged single-substrate 4×4 Butler matrix and double-ridge gap waveguide horn antenna array for multibeam applications," *IEEE Transactions on Microwave Theory and Techniques*, Vol. 69, No. 1, 248–261, 2020.
15. Lee, S., Y. Lee, and H. Shin, "A 28-GHz switched-beam antenna with integrated Butler matrix and switch for 5G applications," *Sensors*, Vol. 21, No. 15, 5128, 2021.
16. Alu, A., M. G. Silveirinha, A. Salandrino, and N. Engheta, "Epsilon-near-zero metamaterials and electromagnetic sources: Tailoring the radiation phase pattern," *Phys. Rev. B*, Vol. 75, No. 15, 155410, 2007.
17. Chen, X., T. M. Grzegorczyk, B.-I. Wu, J. Pacheco, Jr., and J. A. Kong, "Robust method to retrieve the constitutive effective parameters of metamaterials," *Phys. Rev. E*, Vol. 70, No. 1, 016608, 2004.
18. Imani, A. and M. S. Bayati, "A novel design of compact broadband 4×4 Butler matrix-based beamforming antenna array for C-band applications," *AEU — International Journal of Electronics and Communications*, Vol. 138, 153901, 2021.
19. Abdulbari, A. A., S. K. A. Rahim, et al., "A review of hybrid couplers: State-of-the-art, applications, design issues and challenges," *International Journal of Numerical Modelling Electronic Networks Devices and Fields*, Vol. 34, No. 5, e2919, 2021.
20. Balanis, C. A., "Antenna theory: A review," *Proceedings of the IEEE*, Vol. 80, No. 1, 7–23, 1992.